



Gazelle Optimized Visual Geometry Group Network with Resnet101 fostered Oral Squamous Cell Carcinoma Detection

Kumar R^{1,2,*}, S Pazhanirajan³

¹Research Scholar, Department of Computer Science and Engineering, Faculty of Engineering and Technology, Annamalai University, Chidambaram, India

²Assistant Professor, MVJ College of Engineering, Bangalore, India

³Department of Computer Science and Engineering, Faculty of Engineering and Technology, Annamalai University, Chidambaram, India

Emails: rkumarmecse@gmail.com; pazhanisambandam@gmail.com

Abstract

Microscopic examination of tissues to detect oral cancer falls short as traditional microscopes struggle to easily differentiate between cancerous and non-cancerous cells. The identification of cancerous cells through microscopic biopsy images has the potential to alleviate concerns and improve outcomes if precise biological approaches are employed. However, relying solely on physical examinations and microscopic biopsy images for cancer identification increases the likelihood of human error and mistakes. Therefore, in order to obtain accurate results, a new research technique has been developed. In this manuscript, Gazelle Optimized Visual Geometry Group Network with Resnet101 fostered Oral Squamous Cell Carcinoma Detection (OCD-VGGNetCNN-GOA-Resnet101) is proposed. In this method initially, the images are taken from Kaggle repository benchmark dataset and preprocessed to improve image quality. Then the result is given to the Visual Geometry group Network based CNN (VGGNetCNN) with Resnet101 for classification. Finally, the VGGNetCNN -ResNet 101 classifies image into normal and OSCC. Then the simulation performance of the proposed -VGGNetCNN-GOA-Resnet101 method attains 23.67%, 34.89%, 39.45% and 45.31% higher accuracy while compared with existing methods such as OCD-CNN-Alexnet, OCD-CNN-VGG19 and HI-OCD-CNN-INet respectively.

Received: November 04, 2023 Revised: March 23, 2024 Accepted: July 15, 2024

Keywords: Oral squamous cell carcinoma; 2D fast iterative filter; VGGNet; ResNet 101; Gazelle optimization algorithm; Medical imaging

1. Introduction

Based on its high mortality rate, high rate of late diagnoses, and high morbidity rate, the oral cancer is a dangerous disease in the world. Consumption of tobacco products and more alcohol consumption are two main risk factors for oral lesions [1]. The main contributing reason to South and Southeast Asia's high mouth cancer prevalence is betel cigarette use [2]. Tobacco, lime, arecanut, betel leaf is typically included in betel quid [3]. Due to its innovative marketing strategy, betel quid is widely chewed in public [4]. Oral lesions present in later stage, which directly contributes to their low survival rate [5]. Lesion management is expensive, especially in later stages [6]. Medical professionals are concerned because oral lesions are a leading cause of delayed diagnosis and lack of information and public awareness [7]. The characteristics of the lesions is frequently classified as an oral possibly malignant illness. Dental specialists do a clinical oral examination as part of standard screening to diagnose this. When a suspect cancer is found, a professional examination is advised for the patient in order to confirm the diagnosis and provide additional therapy [8]. Previous studies in India have demonstrated that early diagnosis and screening have decreased mortality and morbidity among alcohol and cigarette users [9]. Because of the ongoing shortage of healthcare resources and specialists, screening programs for oral lesions is economical and effectual

[10]. In light of this, telemedicine is a practical sort of technology that can be used for early diagnosis [11]. Due to developments in deep learning (DL) and computer vision, technologies that autonomously check a person's oral cavity then send feedback to medical experts while patient examinations and individual for self-examination are now feasible [12-13]. Prior research has mostly focused auto-fluorescence imaging, hyper spectral imaging, optical coherence tomography to detect oral cancer [14]. While a few researches have used white-light photography, the majority of the older investigations have focused on the recognition of particular kinds of oral lesions [15]. Analysis of the disease's clinical manifestation is insufficient because oral cancer's clinical presentation is insufficient to detect the dysplastic condition. Because the system lacks an automated way to produce accurate image classification results, accuracy and interpretation of the system are highly difficult tasks to complete. In the existing work, during classification, a major limitation is the difficulty in differentiating between normal and OSCC areas, also it possesses low accuracy and high computational time. Human gets affected when there are no accurate results therefore possess a need for the development of new classification algorithms. To overwhelm the issues, some solutions need to be put forward.

Gazelle optimized Visual Geometry Group Network with Resnet101 fostered Oral Squamous Cell Carcinoma Detection is proposed and its contributions are (OCD-VGGNetCNN-GOA-Resnet101).

- Initially, the images are taken from kaggle repository benchmark dataset and pre-processed.
- Input images are pre-processed by 2D fast iterative filter (2DFIF) for eliminating the noise and enhance the image quality.
- These pre-processed images are given to the Visual Geometry group Network based CNN (VGGNetCNN) with Resnet101, here the batch normalization layer of VGGNetCNN is taken away and included with Resnet101layer for enhancing classification.
- Then, Gazelle optimization algorithm is used to optimize VGGNetCNN -ResNet 101 classifier.
- Finally, the VGGNetCNN -ResNet 101 classifies oral cancer into normal and OSCC and also to find the severity of oral lesions.
- Then the proposed OCD-VGGNetCNN-GOA-Resnet101method is analysed and it was compared with the existing methods like Histopathologic Oral Cancer Prediction utilizing OSCC Biopsy Empowered with Transfer Learning (OCD-CNN-Alexnet) [16], Automated categorization of cells as several classes in epithelial tissue of OSCC with the help of transfer learning along CNN (OCD-CNN-VGG19) [17], Automatic Detection of OSCC from Histopathological Images of Oral Mucosa utilizing Deep Convolutional Neural Network(HI-OCD-CNN-INet) [18].

2. Literature Review

Of several studies on Oral Squamous Cell Carcinoma Detection, some of the most recent research works are reviewed here,

Rahman A U., et al., [16] have suggested that Histopathologic Oral Cancer Prediction based upon OSCC Biopsy Empowered with Transfer Learning. If biological approaches were correctly applied for cancerous cells prediction, identification of cancerous cells utilizing microscopic biopsy images aids in defusing as well as predicting the problems and produces better outcomes, but during physical examinations, significant chances for human error. It provides high F1 score and low sensitivity rate. Das N., et al., [17] have suggested automated categorization of cells as several classes in epithelial tissue under transfer learning with CNN. Through the use of pre-trained deep CNN, the study used oral biopsy images to apply transfer learning. Advantage was high accuracy. Dis- advantage was high computational time. Das, M., et al., [18] have presented an research called Automatic identification of OSCC from oral mucosa histopathological images utilizing deep convolutional neural network. Its objective was to examine the effectiveness of the CNN in this specific medical imaging domain. Advantages of this paper are high accuracy. Disadvantages of this paper is high False Positive Ratio.

Marzouk R., et al., [19] have suggested Deep Transfer Learning Driven Oral Cancer identification with categorization method. The presented method includes fuzzy-base contrast development to enable data pre-processing. DenseNet-169 was applied to create valuable set of deep features. It provides high accuracy and low precision rate. Fati S M., et al., [20] have suggested the Early Detection of OSCC depending on Histopathological Images under Deep with Hybrid Learning. The presented model was dependent on hybrid features extracted through AlexNet and ResNet-18consolidated to the color, texture, shape features extracted by fuzzy color histogram, DWT, local binary pattern, GLCM. It provides low computational time with low accuracy. Ono S., et al., [21] have suggested the efficacy of Deep Learning Classifiers in Histopathological detection of OSCC by Pathologists. An oral pathologist prepared oral squamous cell cancer histopathological samples. Furthermore, ROCAUC was considered to statistically assess the enhancement of diagnostic presentation of 6 oral pathologists utilizing the obtained outcomes from CNN method for aided detection.

3. Suggested Approach

Here Gazelle optimized Visual Geometry Group Network with Resnet101 fostered Oral Squamous Cell Carcinoma Detection is proposed (OCD-VGGNetCNN-GOA-Resnet101). The suggested block diagram of OCD-VGGNetCNN-GOA-Resnet101 method is shown in figure 1.

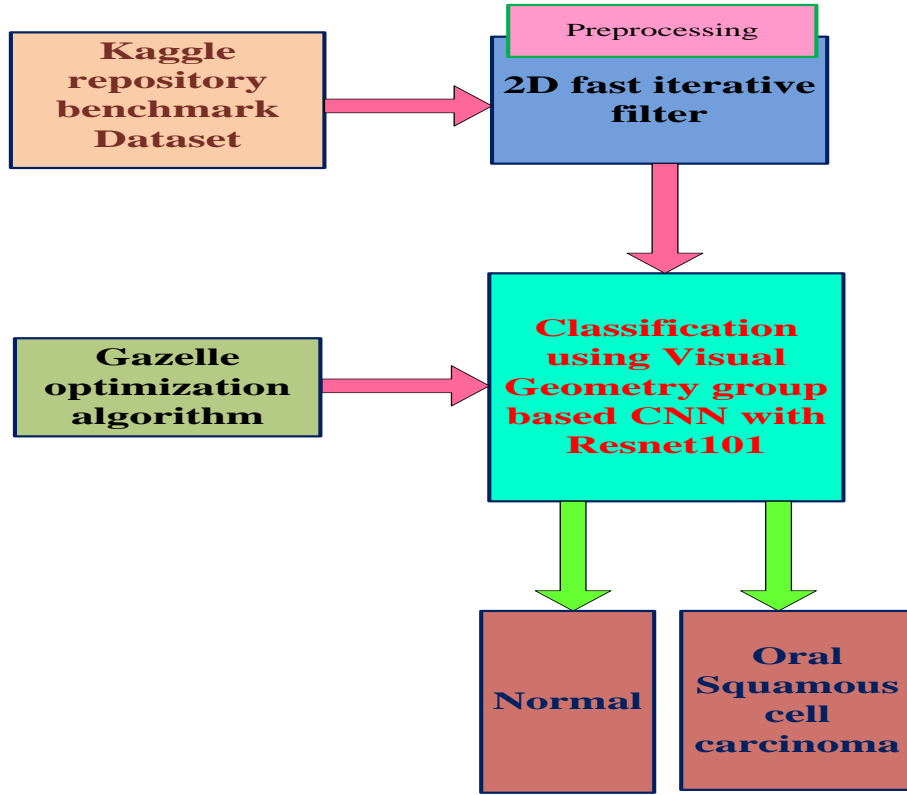


Figure 1. Block diagram of proposedOCD-VGGNetCNN-GOA-Resnet101 Method

A. Image acquisition

Initially, input images are taken from Kaggle repository benchmark dataset [22].It consists of 112,120 images where every image resolution is $1024 * 1024$. Unique patient's images are given by radiological reports and users natural language processors. The dataset covers valuable records such as age, patient data, gender, snapshot data and images.

B. 3.2 Pre-processing using 2D fast iterative filter.

In this step, pre-processed the input images through 2D fast iterative filter (2DFIF) [23] for eradicating the noise and enhancing the image quality. The 2D fast iterative filter typically refers to a computational technique used for image processing. It involves applying an iterative filtering algorithm to a two-dimensional (2D) image to achieve desired filtering effects. The 2D Fast Iterative Filter (2DFIF) is a technique used for removing noise from images and enhancing image quality. It operates by applying a filtering process for achieving high pixel images. To find the pixel value at iteration it is done by using equation (1).

$$I_n(x, y) = I_{True}(x, y) + N_n(x, y) \quad (1)$$

Where (x, y) represents the pixel coordinates, $I_{True}(x, y)$ is denoted as true pixel value, $I_n(x, y)$ is denoted as estimated pixel value at iteration n and $N_n(x, y)$ is denoted as estimated noise at iteration n . Then 2DFIF applies a weight to smooth an image while preserving edges The equation for bilateral filtering at each pixel (x, y) in the 2D image is represented in equation (2)

$$I'(x, y) = \left[\frac{1}{W(x, y)} \sum_{i, j=-k}^k w(x, y, i, j) \times I(x + i, y + j) \right] \quad (2)$$

Where $I'(x, y)$ is denoted as filtered output pixel value at coordinates (x, y) , $W(x, y)$ denotes normalization factor to ensure that the sum of weights is 1, $w(x, y, i, j)$ is denoted as bilateral filter weight for the pixel at $(x + i, y + j)$

and $I(x + i, y + j)$ is denoted as pixel value of the input image. For de-noising the noise in the image it is done by total variation de-noising it is classified using equation (3)

$$\text{Min}_u \lambda = \sqrt{\mathcal{E}^2 + |\nabla u|^2} dx dy + \frac{1}{2} |u - f|^2 dx dy \quad (3)$$

Where u is denoted as de-noised image, λ is denoted as regularization parameter that controls the trade-off between the total variation term and the fidelity term, \mathcal{E} is denoted as small positive value added to the square root to ensure numerical stability and $|\nabla u|$ represents the image gradient. Finally, by using restoring the image it is done by using equation (4)

$$G'(u, v) = \frac{H^*(u, v)}{H^*(u, v) \times H^*(u, v) + \frac{S_n(u, v)}{S_s(u, v)}} \times F(u, v) \quad (4)$$

Where $G'(u, v)$ is denoted as restored image at coordinates (u, v) , $H^*(u, v)$ is denoted as Height of the image function, $S_n(u, v)$ is denoted as width of the image, $S_s(u, v)$ is denoted as noise at coordinates (u, v) and $F(u, v)$ is represented as observed image quality in pixel value. Then the pre processed image is given for classification.

3.3 Classification using Visual Geometry group Network based CNN with Resnet101

In this section, Classification is done using Visual Geometry group Network based CNN with Resnet101. The VGGNetCNN[23] Network gained popularity due to its simplicity and effectiveness in data classification tasks. The key idea behind the VGGNetCNN is to stack multiple layers with small receptive fields (3x3) to increase deep network, which helps in learning complex features. The VGGNetCNN architecture contains 16 weight layers, depending on the variant. The most common variant is VGG, which has 13 convolutional layers as well as 3 fully connected layers. Filters with narrow receptive fields are used in the convolutional layers, and then max-pooling layers are used to down sample the spatial dimensions of the feature maps.

The fully connected layers in the end of VGGNetCNN are responsible for the final classification. The network uses the softmax activation function to assign probabilities to different classes based on the learned features. While the VGGNetCNN achieved excellent results on various data recognition tasks, it has a drawback of being computationally expensive due to its depth and large number of parameters. In addition, VGGNetCNN is combined with an optimization approach like Gazelle optimization algorithm (GOA) to produce the best result for classifying the patient's image as into normal and OSCC. The output feature maps of a convolutional layer is computed using the equation (5),

$$X_i^l = \sigma(X_i^l * X_i^{l-1} + B_i^l) \quad (5)$$

Where X_i^l is denoted as output of the Convolutional layer, X_i^{l-1} is denoted as input feature map from the previous layer, B_i^l is denoted as bias term. Next Max-pooling layer is needed in the VGGNetCNN, while the maps of a max-pooling layer output can be obtained by selecting the maximum value within a pooling region. The max-pooling layer output is denoted in equation (6)

$$Y^l = \sigma[W^l X^{l-1} + B^l] \quad (6)$$

Where Y^l represents max-pooling layer output, W^l represents the weight matrix, W^{l-1} is denoted as the input vector of the previous layer and B_i^l is denoted as bias term. Max-pooling layer is acquired by selecting the maximal value within a pooling region. The equation is derived by using equation (7)

$$X_i^l = \text{Max}(X_i^{l-1}) \quad (7)$$

Where i is denoted as the Max pooling layer, l is denoted as maximum value within a pooling region from the input feature map X_i^l . Then by using this ReLU activation function in VGGNetCNN it is commonly used to introduce non-linearity by using equation (8)

$$\text{ReLU}(x) = \text{Max}(0, x) \quad (8)$$

here the ReLU function applies element-wise to each neuron's output in VGGNetCNN layer, setting any negative values to zero and keeping positive values unchanged the layer is placed. Next is Softmax activation function is used. The softmax function calculates the exponential of each element in a vector of real values that it receives as input. Resulting values are normalized by dividing each exponential value by the sum of all exponential values, ensuring that the resulting values sum up to 1. The output of the softmax layer is derived by using equation (9)

$$Y_{\text{out}} = \left[\frac{\text{Exp}(y)}{(\text{Exp}(x_1) + \text{Exp}(x_2) + \dots + \text{Exp}(x_n))} \right] \quad (9)$$

Where Y_{out} is denoted as the derived output of softmax layer, x is denoted as input vector and y is denoted as output vector. In classification problems, the cross-entropy loss function is used to scale the difference between anticipated and actual class probabilities. So to find the loss value is important and it is derived using equation (10)

$$Loss = -\sum_i [y_i \log(\hat{y}_i)] \quad (10)$$

Where y_i denotes the true class probabilities and \hat{y}_i is known as difference between the loss values. Then the Backpropagation for weight updates in a neural network are updated using the backpropagation value. The weight update equation is mentioned using equation (11)

$$\Delta W_i^l = \left[-\eta \frac{\delta Loss}{\delta W_i^l} \right] \quad (11)$$

Where ΔW_i^l is denoted as the updated weight, η is denoted as the learning rate of VGGNetCNN layer. In this, Visual Geometry group Network based CNN shows better classification performance but for classification over fitting problem occurs in the images, so the VGGNetCNN batch normalization layer is eliminated and added to Resnet101. ResNet101 [24] effectively train very deep neural networks by addressing the problem of vanishing gradients. ResNet101 lies in the use of residual connections and it able to skip connections. With the help of these connections, the network is able to learn residual mappings, which capture residual variation between the input and the intended output.

By propagating the residual information through the network, ResNet101 overcomes the degradation problem associated with training very deep neural networks. The skip connections also enable the gradients to flow more easily during backpropagation, addressing the issue of vanishing gradients and making it easier to train deep models. ResNet101 architecture consists of several residual blocks, each one contains multiple convolutional layers. These blocks are grouped together to form different stages, gradually reducing the spatial dimensions while increasing the number of filters. The network utilizes bottleneck structures to reduce computational complexity. This approach balances model depth and computational efficiency. In ResNet-101, global average pooling is typically applied to convert the spatial feature maps into a one-dimensional vector. To find the global average pooling it is explained in equation (12)

$$Z = \frac{1}{H \times W} \sum_{ij=1}^{HW} X_{ij} \quad (12)$$

X_{ij} is denoted as feature map values at spatial location, H and W are denoted as height and width of the feature maps. Batch normalization is commonly used in ResNet-101 to normalize the activations within each mini-batch. The equation for batch normalization is given in equation (13)

$$Y = \left[\frac{X - \mu}{\sqrt{\sigma^2 + \xi}} \right] * \gamma + \beta \quad (13)$$

Hence Y is denoted as batch normalization output, X is denoted as input of batch normalization layer, σ^2 is denoted as mean and variance of mini-batch, γ and β are known as learnable scale, shift parameters. Finally, VGGNetCNN -ResNet 101 classifies oral cancer into normal and OSCC. And also for getting better accuracy the weight parameters of the result of VGGNetCNN -ResNet 101 is given for Gazelle optimization algorithm (GOA).

3.4 Gazelle optimization algorithm

Gazelle optimization algorithm [25] optimize the weight parameters of Visual Geometry group Network based CNN with Resnet101. The optimization is done in two parameters because of problems in VGGNetCNN -ResNet 101. So the two weight parameters of VGGNetCNN -ResNet 101 is given to Gazelle optimization algorithm for optimization. Gazelle optimization algorithm is a metaheuristic optimization approach inspired by the behaviour of gazelles in nature. Each gazelle specifies a potential solution to the optimization problem and moves through the search space in search of better solutions. The movement of gazelles is influenced by their own previous best position, the global best position found by the entire herd, and the positions of neighbouring gazelles. The algorithm incorporates various adaptive mechanisms and exploration-exploitation strategies to balance exploration of the search space and exploitation of promising regions. It utilizes the concept of speed, position, and acceleration to update the positions of gazelles, similar to how the physical attributes of real gazelles affect their movements. These behaviours enhance the convergence speed and help the escape of the algorithm from local optima. Additionally, gazelles are encouraged to explore unvisited search space areas to ensure global search capability. Overall the unique characteristics of gazelles to provide an efficient and robust optimization approach. It has been applied to various optimization issues, like engineering design, scheduling, machine learning, demonstrating its effectiveness for defining high-quality solutions. Here weight parameters in the Visual Geometry group Network based CNN with Resnet101 have parameters of X_i^{l-1} and η are optimized using Gazelle optimization algorithm.

The stages in GOA approaches are as follows:

Step 1: Initialization

The Initial population is used by GOA and generated stochastically between the given problem's upper bound (UB) and lower bound (LB) is activated. The weight parameters of the VGGNetCNN – ResNet) is optimized by initialize the candidate population of the gazelles. Therefore, the current candidate's position is given in equation (14)

$$Y = \begin{bmatrix} y_{1,1}y_{1,2}...y_{1,e-1}y_{1,e} \\ y_{1,1}y_{1,2}...y_{1,e-1}y_{1,e} \\ y_{ij} \\ y_{o,1}y_{o,2}...y_{o,e-1}y_{o,e} \end{bmatrix} \quad (14)$$

Where Y is denoted as total current candidate position, Y_{ij} denotes position of j^{th} population and i^{th} dimension, o is denoted as current candidate population and e is denoted as dimension.

Step 2: Random generation

After start up, the loop's parameters were created at random. The value of optimal fitness is selected taking into account their specific hyper parameter conditions.

Step 3: Estimation of Fitness Function

The random solution is produced from the initialization. The fitness function is appraised with the values of parameter optimization for optimizing weight parameter X_i^{l-1} and η of VGGNetCNN –ResNet 101. Hence, the fitness function is expressed in equation (15)

$$FitnessFunction = optimizing[X_i^{l-1} and \eta] \quad (15)$$

Step 4: Exploration stage for optimizing X_i^{l-1} and η

When a predator is seen, the exploring phase begins. When faced with danger, gazelles stomp their feet and flick their tail and adopt a leaping style known as "stotting," which involves springing into the air up to a height of two meter with all four feet. They update their direction according to X_i^{l-1} and η . This is expressed in equation (16)

$$z_{bo}(l) = z_{bo}(l + \beta 1 * [z_{best}(l) - z_{bestup}(l)]) \quad (16)$$

Where z_{bo} is the population member who is adolescence, z_{bestup} signifies current best group member position, z_{best} represents current best optimal solution, and $\beta 1$ denotes random integer drawn at random from a uniform distribution.

Step 5: Termination Condition

In this step, the weight parameter values X_i^{l-1} and η of VGGNetCNN –ResNet 101 are optimized with the help of GOA Algorithm otherwise the algorithm repeat step 3 until fulfill the halting criteria $g = g + 1$. Lastly, VGGNetCNN –ResNet 101 with GOA algorithm identifies the Image into normal and Oral Squamous cell carcinoma (OSCC)

4. Findings and Discussion

In this section a Gazelle Optimized Visual Geometry Group Network with Resnet101 fostered Oral Squamous Cell Carcinoma Detection (OCD-VGGNetCNN-GOA-Resnet101). Measurements such as accuracy, F-Score, ROC and Computation time are verified. The performance of the proposed OCD-VGGNetCNN-GOA-Resnet101 is compared with existing methods such as OCD-CNN-Alexnet, OCD-CNN-VGG19 and HI-OCD-CNN-INet respectively.

4.1 Performance Measures

Performance measurements are discussed below.

4.1.1 Accuracy

The accuracy is measured as the ratio of a correct forecast to the total number of proceedings

(equation 17).

$$Accuracy = \frac{TP+TN}{TP+TN+FP+FN} \quad (17)$$

TP Denotes true positive, TN signifies true negative, FP specifies false positive, FN specifies false negative.

4.1.2 F-score

This is determined by equation (18),

$$F - Scorevalue = \frac{TP}{TP + \frac{1}{2}(FP+FN)} \quad (18)$$

4.1.3 ROC

Roc gives insight and its clearance rate from the body is expressed in equation (19)

$$ROC = 0.5 \times \left(\frac{TP}{TP+FN} + \frac{TN}{TN+FP} \right) \quad (19)$$

4.1.4 Computation time

After startup, the loop's parameters were created at random. The value of optimal fitness is selected taking into account their specific hyper parameter conditions. It is shown in equation (20).

$$Computationtime = \frac{W_c * WCF}{ClockRate} \quad (20)$$

Where W_c is denoted as clock cycles, WCF is said as instruction count in clock cycle.

4.2 Comparison of performance analysis

Here, the performance analysis for detecting image into normal and Oral Squamous cell carcinoma (OSCC) are analysed. Performance analysis such as accuracy, sensitivity, precision and specificity are analysed with existing models. The performance analysis of OCD-VGGNetCNN-GOA-Resnet101 is shown in table 1.

Table 1: Performance analysis for OCD-VGGNetCNN-GOA-Resnet101

Methods	Accuracy (%)		F-Score (%)		Computational Time (s)
	Normal	Oral Squamous cell carcinoma	Normal	Oral Squamous cell carcinoma	
OCD-CNN-Alexnet	55.37	60.44	65.44	63.55	54.22
OCD-CNN-VGG19	70.33	56.66	56.77	43	48.44
HI-OCD-CNN-INet	74.69	40	65.36	36.44	50.45
OCD-VGGNetCNN-GOA-Resnet101(Proposed)	99.13	99.37	99.22	99.04	22.23

Table 1 depicts the performance of accuracy; F-Score, ROC and Computation time are verified.

The accuracy of proposed OCD-VGGNetCNN-GOA-Resnet101 method attains in normal 23.67%, 34.89%, and 39.45%, higher accuracy; in Oral Squamous cell carcinoma 28.23%, 31.34%, and 36.07%, higher accuracy. The F-Score of proposed method attains in normal 33.12%, 28.12%, and 34.12% higher F-Score; in Oral Squamous

cell carcinoma 22.32%, 35.44%, and 36.12% higher F-Score. The Computational time of proposed method attains 28.15%, 22.39%, and 35.33% lower Computational time while compared with existing methods such as OCD-CNN-Alexnet, OCD-CNN-VGG19 and HI-OCD-CNN-INet respectively.

Figure 2 depicts ROC analyses. The proposed OCD-VGGNetCNN-GOA-Resnet101 method attains 33.40%, 24.12% and 27.22% high false rate. And the outcomes are comparing the existing methods such as OCD-CNN-Alexnet, OCD-CNN-VGG19 and HI-OCD-CNN-INet respectively.

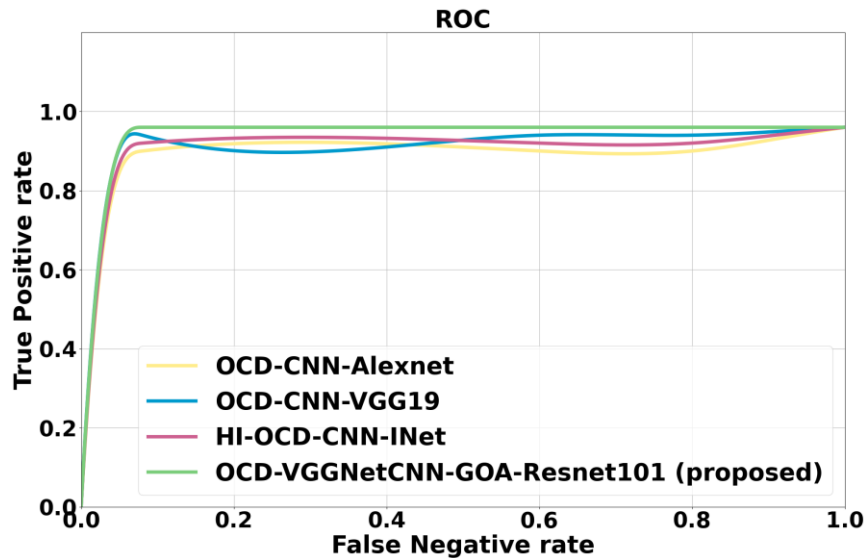


Figure 2. False Negative Rate Analysis

5. Conclusion

In this research work, Gazelle Optimized Visual Geometry Group Network with Resnet101 fostered Oral Squamous Cell Carcinoma Detection (OCD-VGGNetCNN-GOA-Resnet101) is proposed. Measurements like accuracy, sensitivity, precision and specificity are examined. Then the proposed OCD-VGGNetCNN-GOA-Resnet101 technique shows 28.15%, 22.39%, and 35.33% lower Computational time while compared with existing OCD-CNN-Alexnet, OCD-CNN-VGG19 and HI-OCD-CNN-INet methods respectively. This article gives linear model, which is the direct simplex method using neutrosophic logic, the logic that is the new vision of modelling and is designed to effectively address the uncertainties inherent in the real world founded by the Romanian mathematician Florentine Smarandache [1, 2]. In addition to that, Ahmed A. Salama presented the theory of neutrosophic classical categories as a generalization of the theory of classical categories [12,20], also, he developed, introduced, and formulated new concepts in the various disciplinary of mathematics, statistics, computer science by neuromorphic theory [17,18,19,22,28].

Funding: "This research received no external funding"

Conflicts of Interest: "The authors declare no conflict of interest."

References

- [1] Warnakulasuriya, S., Kujan, O., Aguirre-Urizar, J.M., Bagan, J.V., González-Moles, M.Á., Kerr, A.R., Lodi, G., Mello, F.W., Monteiro, L., Ogden, G.R. and Sloan, P., 2021. Oral potentially malignant disorders: A consensus report from an international seminar on nomenclature and classification, convened by the WHO Collaborating Centre for Oral Cancer. *Oral diseases*, 27(8), pp.1862-1880.
- [2] Vimala, S. Krishnan, V. Raj, M. Kumar, A. Janakiraman, M. "Object Detection Using Deep Learning," *Journal of Journal of Cognitive Human-Computer Interaction*, vol. 6, no. 1, pp. 32-38, 2023. DOI: <https://doi.org/10.54216/JCHCI.060103>
- [3] Awais, M., Ghayvat, H., Krishnan Pandarathodiyil, A., Nabillah Ghani, W.M., Ramanathan, A., Pandya, S., Walter, N., Saad, M.N., Zain, R.B. and Faye, I., 2020. Healthcare professional in the loop (HPIL): classification of standard and oral cancer-causing anomalous regions of oral cavity using textural analysis technique in autofluorescence imaging. *Sensors*, 20(20), p.5780.

- [4] Rajan, J.P., Rajan, S.E., Martis, R.J. and Panigrahi, B.K., 2020. Fog computing employed a computer aided cancer classification system using deep neural network in internet of things-based healthcare system. *Journal of medical systems*, 44, pp.1-10.
- [5] Alabi, R.O., Elmusrati, M., Sawazaki-Calone, I., Kowalski, L.P., Haglund, C., Coletta, R.D., Mäkitie, A.A., Salo, T., Almangush, A. and Leivo, I., 2020. Comparison of supervised machine learning classification techniques in prediction of locoregional recurrences in early oral tongue cancer. *International journal of medical informatics*, 136, p.104068.
- [6] Palaskar, R., Vyas, R., Khedekar, V., Palaskar, S. and Sahu, P., 2020. Transfer learning for oral cancer detection using microscopic images. *arXiv preprint arXiv:2011.11610*.
- [7] Das, N., Hussain, E. and Mahanta, L.B., 2020. Automated classification of cells into multiple classes in epithelial tissue of oral squamous cell carcinoma using transfer learning and convolutional neural network. *Neural Networks*, 128, pp.47-60.
- [8] Jubair, F., Al-karadsheh, O., Malamos, D., Al Mahdi, S., Saad, Y. and Hassona, Y., 2022. A novel lightweight deep convolutional neural network for early detection of oral cancer. *Oral Diseases*, 28(4), pp.1123-1130.
- [9] Sarode, G., Maniyar, N., Sarode, S.C., Jafer, M., Patil, S. and Awan, K.H., 2020. Epidemiologic aspects of oral cancer. *Disease-a-Month*, 66(12), p.100988.
- [10] Panigrahi, S., Das, J. and Swarnkar, T., 2022. Capsule network-based analysis of histopathological images of oral squamous cell carcinoma. *Journal of King Saud University-Computer and Information Sciences*, 34(7), pp.4546-4553.
- [11] Xue, Z., Pearlman, P.C., Yu, K., Pal, A., Chen, T.C., Hua, C.H., Kang, C.J., Chien, C.Y., Tsai, M.H., Wang, C.P. and Chaturvedi, A.K., 2022, April. Oral cavity anatomical site image classification and analysis. In *Medical Imaging 2022: Imaging Informatics for Healthcare, Research, and Applications* (Vol. 12037, pp. 90-96). SPIE.
- [12] Song, B., Sunny, S., Li, S., Keerthi, G., Patrick, S., Mukhia, N., Gurudath, S., Raghavan, S., Mendonca, P., Leivon, S.T. and Kolur, T., 2020, September. Reliable Oral Cancer Classification Framework with Bayesian Deep Learning. In *Laser Science* (pp. JM6B-18). Optica Publishing Group.
- [13] Edin, N. "Towards Efficient Hyperspectral Object Detection and Classification using Thermal Optimization Algorithm with Deep Learning," *Journal of International Journal of Advances in Applied Computational Intelligence*, vol. 6, no. 2, pp. 1-15, 2024. DOI: <https://doi.org/10.54216/IJAACI.060201>
- [14] Alanazi, A.A., Khayyat, M.M., Khayyat, M.M., ElaminElnaim, B.M. and Abdel-Khalek, S., 2022. Intelligent Deep Learning Enabled Oral Squamous Cell Carcinoma Detection and Classification Using Biomedical Images. *Computational Intelligence and Neuroscience*, 2022.
- [15] Panigrahi, S., Nanda, B.S. and Swarnkar, T., 2022. Comparative analysis of machine learning algorithms for histopathological images of oral cancer. In *Advances in Distributed Computing and Machine Learning: Proceedings of ICADCML 2021* (pp. 318-327). Springer Singapore.
- [16] [Rahman, A.U., Alqahtani, A., Aldhafferi, N., Nasir, M.U., Khan, M.F., Khan, M.A. and Mosavi, A., 2022. Histopathologic oral cancer prediction using oral squamous cell carcinoma biopsy empowered with transfer learning. *Sensors*, 22(10), p.3833.
- [17] Das, N., Hussain, E. and Mahanta, L.B., 2020. Automated classification of cells into multiple classes in epithelial tissue of oral squamous cell carcinoma using transfer learning and convolutional neural network. *Neural Networks*, 128, pp.47-60.
- [18] Das, M., Dash, R. and Mishra, S.K., 2023. Automatic detection of oral squamous cell carcinoma from histopathological images of oral mucosa using deep convolutional neural network. *International Journal of Environmental Research and Public Health*, 20(3), p.2131.
- [19] Marzouk, R., Alabdulkreem, E., Dhahbi, S., Nour, M.K., Duhayyim, M.A., Othman, M., Hamza, M.A., Motwakel, A., Yaseen, I. and Rizwanullah, M., 2022. Deep Transfer Learning Driven Oral Cancer Detection and Classification Model. *Computers, Materials & Continua*, 73(2).
- [20] S. M. Fati, E. M. Senan, and N. ElHakim, "Early Diagnosis of Oral Squamous Cell Carcinoma Based on Histopathological Images Using Deep and Hybrid Learning Approaches," *Applied Sciences*, vol. 12, no. 14, p. 7092, 2022. DOI: 10.3390/app12147092.
- [21] Sukegawa, S., Ono, S., Tanaka, F., Inoue, Y., Hara, T., Yoshii, K., Nakano, K., Takabatake, K., Kawai, H., Katsumitsu, S. and Nakai, F., 2023. Effectiveness of Deep Learning Classifiers in Histopathological Diagnosis of Oral Squamous Cell Carcinoma by Pathologists.
- [22] <https://www.kaggle.com/general/248718>

- [23] Rogalski, M., Pielach, M., Cicone, A., Zdańkowski, P., Stanaszek, L., Drela, K., Patorski, K., Lukomska, B. and Trusiak, M., 2022. Tailoring 2D fast iterative filtering algorithm for low-contrast optical fringe pattern preprocessing. *Optics and Lasers in Engineering*, 155, p.107069.
- [24] Vharkate, M.N. and Musande, V.B., 2021. Remote sensing image retrieval using hybrid visual geometry group network with relevance feedback. *International Journal of Remote Sensing*, 42(14), pp.5540-5567.
- [25] Lin, S.L., 2021. Application combining VMD and ResNet101 in intelligent diagnosis of motor faults. *Sensors*, 21(18), p.6065.
- [26] Agushaka, J.O., Ezugwu, A.E. and Abualigah, L., 2023. Gazelle Optimization Algorithm: A novel nature-inspired metaheuristic optimizer. *Neural Computing and Applications*, 35(5), pp.4099-4131.